

Chemical and Electrochemical Oxidation of $\text{CpRe}(\text{PAr}_3)_2\text{H}_2$ Complexes To Give Stable 17-Electron Radical Cations. Disproportionation to Diamagnetic Species via Electron-Transfer Catalysis

Michael R. Detty*[†] and William D. Jones*[‡]

Contribution from the Corporate Research Laboratories, Eastman Kodak Company, Rochester, New York 14650, and Department of Chemistry, University of Rochester, Rochester, New York 14627. Received January 30, 1987

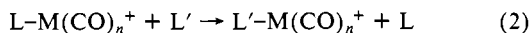
Abstract: Oxidations of $\text{CpRe}(\text{PAr}_3)_2\text{H}_2$ complexes give stable $[\text{CpRe}(\text{PAr}_3)_2\text{H}_2]^{+\bullet}$ complexes in both acetonitrile and dichloromethane as determined by controlled-potential thin-layer coulometry and double-potential step chronocoulometry. The magnitude of E° for the Re(III)/Re(IV) couple as determined by cyclic voltammetry is influenced by the aryl substituents in the $\text{CpRe}[\text{P}(p\text{-XC}_6\text{H}_4)_3]_2$ complexes (1: X = H; 3: X = Me; 4: X = F; 5: X = MeO) with E° becoming more positive as the σ -donating ability of the substituent decreases. Oxidation at more positive potentials presumably produces $[\text{CpRe}(\text{PAr}_3)_2\text{H}_2]^{2+}$, a diamagnetic 16-electron species, which reacts with the 17-electron species. This reaction is autocatalytic with the electron-transfer catalysis (ETC), giving current efficiencies of between 5 and 20 for each electron removed beyond the 17-electron species. In acetonitrile, the reaction driven by ETC gave equal amounts of two products, $[\text{CpRe}(\text{PAr}_3)_2(\text{NCCH}_3)\text{H}]^+$ and $[\text{CpRe}(\text{PAr}_3)_2\text{H}_3]^+$, while in dichloromethane only the latter product was produced. Ferricinium hexafluorophosphate oxidation of 1 gave $[\text{CpRe}(\text{PPh}_3)_2(\text{NCCH}_3)\text{H}]^+[\text{PF}_6]^-$ (7) in 43% yield and $[\text{CpRe}(\text{PPh}_3)_2\text{H}_3]^+[\text{PF}_6]^-$ in 45% yield. The structure of 7 was determined unambiguously by single-crystal X-ray crystallographic analysis. The molecule $[\text{CpRe}(\text{PPh}_3)_2(\text{NCCH}_3)\text{H}]^+[\text{PF}_6]^-$ crystallizes in a trans geometry in monoclinic space group $P2_1/c$ with $Z = 4$, $a = 9.908$ (2) Å, $b = 21.546$ (9) Å, $c = 18.967$ (6) Å, and $\beta = 99.12$ (2)°. The $[\text{CpRe}(\text{PAr}_3)_2(\text{NCCH}_3)\text{H}]^+$ complexes exhibit reversible one-electron oxidations by cyclic voltammetry and show that the magnitude of E° is once more a function of the electron-donating ability of the aryl substituents. The mechanism of chain propagation in the reactions of the $[\text{CpRe}(\text{PAr}_3)_2\text{H}_2]^{+\bullet}$ complexes involves either proton transfer or hydrogen atom transfer with the 16-electron $[\text{CpRe}(\text{PAr}_3)_2\text{H}_2]^{2+}$ moieties to give species capable of oxidizing more of the 17-electron complex.

Odd-electron, paramagnetic intermediates with 15-, 17-, and 19-electron configurations are becoming increasingly important in transition-metal reactions.² Such species have been studied as persistent radicals³ or as transient species generated by metal-metal bond dissociation,⁴ photochemical reduction,⁵ or chemical-electrochemical oxidation-reduction⁶ of suitable precursors. The mechanism of ligand substitution reactions in paramagnetic intermediates is of interest because their rates of reaction are often many orders of magnitude faster than in diamagnetic complexes with 16- and 18-electron configurations.³ Substitution reactions in paramagnetic complexes of metal carbonyls have been most frequently studied. Substitution of $\text{Mn}(\text{CO})_5$ has been found to be associative,⁷ while chain processes involving 17-electron radical cations have been implicated in many other metal carbonyl derivatives.^{6d,h,i}

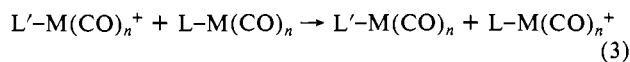
In ligand substitution reactions of metal carbonyl derivatives that are driven by chain processes involving 17-electron radical cations, three discrete reactions have been identified.^{6d} The first (eq 1) is the chemical or electrochemical oxidation of the metal carbonyl complex.



The second reaction (eq 2) is ligand substitution.



Finally, the chain is propagated by an electron-transfer step (eq 3).



This last step must generate a species capable of oxidizing the starting metal carbonyl complex for electron-transfer catalysis (ETC)⁸ to occur. In those cases where ETC efficiencies have been measured, turnover numbers of greater than 10^3 have been observed for each electron removed.^{6d,e}

Organometallic complexes of rhenium have been of interest for their ability to form electron-rich coordinatively unsaturated intermediates upon photolysis that give catalytic H/D exchange between alkanes and arenes.⁹ Ligand substitution in these

(1) A. P. Sloan Fellow, 1984-1986; Camille and Henry Dreyfuss, Teacher Scholar, 1985-1987.

(2) (a) Kochi, J. K. *Organometallic Mechanisms and Catalysis*; Academic: New York, 1978. (b) Kochi, J. K. *Acc. Chem. Res.* **1974**, *7*, 351. (c) Brown, T. L. *Ann. N.Y. Acad. Sci.* **1980**, *80*. (d) Lappert, M. F.; Lednor, P. W. *Adv. Organomet. Chem.* **1976**, *14*, 345. (e) Espenson, J. H. *Prog. Inorg. Chem.* **1983**, *30*, 189.

(3) Shi, Q.-Z.; Richmond, T. G.; Trogler, W. C.; Basolo, F. *J. Am. Chem. Soc.* **1984**, *106*, 71.

(4) (a) Byers, B. H.; Brown, T. L. *J. Am. Chem. Soc.* **1975**, *97*, 3260. (b) Absi-Halabi, M.; Brown, T. L. *Ibid.* **1977**, *99*, 2982. (c) Kidd, D. R.; Brown, T. L. *Ibid.* **1978**, *100*, 4095. (d) Kidd, D. R.; Chang, C. P.; Brown, T. L. *Ibid.* **1978**, *100*, 4103. (e) McCullen, S. B.; Brown, T. L. *Inorg. Chem.* **1981**, *20*, 3528. (f) Haines, L. I. B.; Hoggood, D.; Poe, A. J. *J. Chem. Soc. A* **1968**, 421. (g) Fawcett, J. P.; Jackson, R. A.; Poe, A. J. *J. Chem. Soc.* **1975**, 733. (h) Fawcett, J. P.; Jackson, R. A.; Poe, A. J. *J. Chem. Soc., Dalton Trans.* **1978**, 789. (i) Fox, A.; Malito, J.; Poe, A. *J. Chem. Soc., Chem. Commun.* **1981**, 1052. (j) Wrighton, M. S.; Ginley, D. S. *J. Am. Chem. Soc.* **1975**, *97*, 2065. (k) Hepp, A. F.; Wrighton, M. S. *Ibid.* **1983**, *105*, 5934. (l) Muetterties, E. L.; Sosinsky, B. A.; Zamaraev, K. I. *Ibid.* **1975**, *97*, 5299. (m) Mirbach, M. F.; Mirbach, M. J.; Wegman, R. W. *Organometallics* **1984**, *3*, 900.

(5) Summers, D. P.; Luong, J. C.; Wrighton, M. S. *J. Am. Chem. Soc.* **1981**, *103*, 5238.

(6) (a) Allison, J. D.; Cameron, C. J.; Wild, R. E.; Walton, R. A. *J. Organomet. Chem.* **1981**, *218*, C62. (b) Allison, J. D.; Walton, R. A. *J. Chem. Soc., Chem. Commun.* **1983**, 401. (c) Asaro, M. F.; Bodner, G. S.; Gladysz, J. A.; Cooper, S. R.; Cooper, N. J. *Organometallics* **1985**, *4*, 1020. (d) Zizelman, P. M.; Amatore, C.; Kochi, J. K. *J. Am. Chem. Soc.* **1984**, *106*, 3771. (e) Hershberger, J. W.; Klingler, R. J.; Kochi, J. K. *Ibid.* **1983**, *105*, 61. (f) Narayanan, B. A.; Amatore, C.; Kochi, J. K. *J. Chem. Soc., Chem. Commun.* **1983**, 397. (g) Hershberger, J. W.; Amatore, C.; Kochi, J. K. *J. Organomet. Chem.* **1983**, *250*, 345. (h) Hershberger, J. W.; Klingler, R. J.; Kochi, J. K. *J. Am. Chem. Soc.* **1982**, *104*, 3034. (i) Hershberger, J. W.; Kochi, J. K. *J. Chem. Soc., Chem. Commun.* **1982**, 212. (j) Bowyer, W. J.; Geiger, W. E.; Boekelheide, V. *Organometallics* **1984**, *3*, 1079. (k) Darchen, A. *J. Chem. Soc., Chem. Commun.* **1983**, 768. (l) Krusic, P. J.; San Filippo, J., Jr. *J. Am. Chem. Soc.* **1982**, *104*, 2645. (m) Nesmeyanov, A. N.; Vol'kenau, N. A.; Shilovtseva, L. S. *J. Organomet. Chem.* **1973**, *61*, 329. (n) Asaro, M. A.; Cooper, S. R.; Cooper, N. J. *J. Am. Chem. Soc.* **1986**, *108*, 5187.

(7) (a) Herrinton, T. R.; Brown, T. L. *J. Am. Chem. Soc.* **1985**, *107*, 5700.

(b) Turaki, N. N.; Huggins, J. M. *Organometallics* **1986**, *5*, 1703.

(8) Chanon, M. *Bull. Soc. Chim. Fr.* **1982**, II-197.

[†] Eastman Kodak Company.

[‡] University of Rochester.

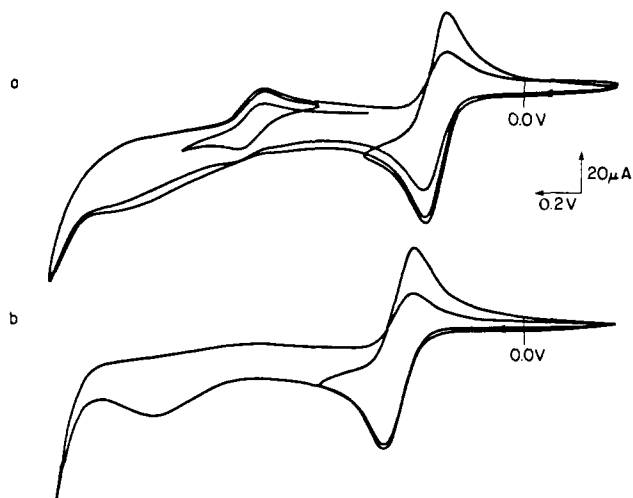


Figure 1. Cyclic voltammograms of 5.0×10^{-4} M $\text{CpRe}(\text{P}(p\text{-FC}_6\text{H}_4)_2)_2\text{H}_2$ (**4**) in (a) acetonitrile and (b) dichloromethane with 0.2 M tetrabutylammonium fluoroborate as supporting electrolyte at a platinum disk electrode and a sweep rate of 0.1 V s^{-1} .

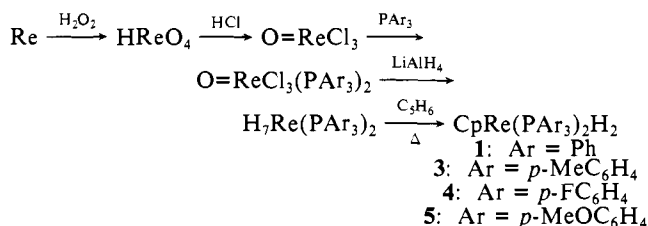
complexes, $\text{CpRe}(\text{PPh}_3)_2\text{H}_2$ (**1**),^{9a,b} $(\eta^6\text{-C}_6\text{H}_6)\text{Re}(\text{PPh}_3)_2\text{H}_2$,^{9c} and $\text{ReH}_3(\text{diphos})_2$ (diphos = $\text{Ph}_2\text{PCH}_2\text{CH}_2\text{PPh}_2$),^{9d} is thermally quite slow, and phosphine dissociation proceeds only by photochemical means, making derivatives of these systems somewhat troublesome to prepare.

We were interested in the possibility of preparing derivatives of **1** by using paramagnetic intermediates to accelerate substitution reactions in **1**. The dinuclear rhenium polyhydrides have been found to give stable radical cations upon oxidation.^{6a,b} Furthermore, ligand-substitution reactions were found to be much faster in the radical cations than in the diamagnetic precursors. The mononuclear rhenium alkyls $\text{CpRe}(\text{NO})(\text{PPh}_3)\text{R}$ (**2**) give partially reversible oxidations by cyclic voltammetry,^{6c} suggesting that the $\text{CpRe}(\text{NO})(\text{PPh}_3)\text{R}^+$ 17-electron species has some stability. The similarity in structure between **1** and **2** prompted us to examine the electrochemical behavior of **1** and related compounds. We report here the results of that study, which include the isolation of stable 17-electron intermediates as well as an example of ETC driving the disproportionation of stable 17-electron rhenium(IV) species.

Results and Discussion

Preparation of Materials. Complex **1** has been prepared by the route shown in Scheme I.¹⁰ We were interested in varying the phosphine ligands in **1** to examine the effect of ligands on the redox potentials of the complex. The known complexes **3** and **4**^{10c} as well as the new complex **5** were all prepared according to Scheme I, although $\text{O}=\text{ReCl}_3[\text{P}(p\text{-MeOPh})_3]_2$ was prepared in higher yield by the exchange of $\text{P}(p\text{-MeOPh})_3$ for PPh_3 in $\text{O}=\text{ReCl}_3(\text{PPh}_3)_2$ than by the reaction of $\text{P}(p\text{-MeOPh})_3$ with HReO_4 and HCl.

Scheme I



(9) (a) Jones, W. D.; Maguire, J. A. *Organometallics* **1986**, *5*, 590. (b) Jones, W. D.; Maguire, J. A. *J. Am. Chem. Soc.* **1985**, *107*, 4544. (c) Jones, W. D.; Fan, M. *Organometallics* **1986**, *5*, 1057. (d) Bradley, M. G.; Roberts, D. A.; Geoffroy, G. L. *J. Am. Chem. Soc.* **1981**, *103*, 379.
(10) (a) Baudry, D.; Ephritikhine, M. *J. Chem. Soc., Chem. Commun.* **1980**, 249. (b) Baudry, D.; Ephritikhine, M.; Felkin, H. *J. Organomet. Chem.* **1982**, *224*, 1663. (c) Baudry, D.; Ephritikhine, M.; Felkin, H. *J. Chem. Soc., Chem. Commun.* **1982**, 606.

Table I. Reversible CV Parameters of $\text{CpRe}(\text{P}(\text{Ar})_3)_2\text{H}_2$ Complexes^a

entry	compd	solvent	E_p^a , V ^b	$(E_p^a - E_p^c)/2$, V ^b	i_p^a/i_p^c
1	1	CH_3CN	0.26	0.23	1.1
2	1	CH_2Cl_2	0.29	0.25	1.2
3	3	CH_3CN	0.12	0.09	1.0
4	3	CH_2Cl_2	0.175	0.14	1.0
5	4	CH_3CN	0.33	0.30	1.1
6	4	CH_2Cl_2	0.41	0.37	1.1
7	5	CH_3CN	0.09	0.06	1.0
8	5	CH_2Cl_2	0.13	0.09	1.0

^aSolutions were 5×10^{-4} M in the complex with 0.2 M TBAF as supporting electrolyte at a platinum disk electrode with a scan rate of 100 mV s^{-1} . ^bvs. SCE.

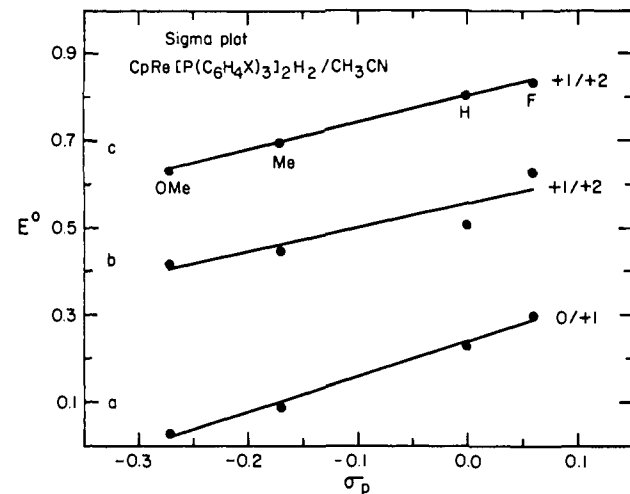
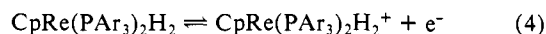


Figure 2. Plot of E^0 vs. σ_p for the substituents X in the oxidation in acetonitrile of (a) $\text{CpRe}(\text{P}(p\text{-XC}_6\text{H}_4)_2)_2\text{H}_2$, (b) $[\text{CpRe}(\text{P}(p\text{-XC}_6\text{H}_4)_2)_2\text{H}_2]^+$, and (c) $[\text{CpRe}(\text{P}(p\text{-XC}_6\text{H}_4)_2)(\text{NCCH}_3)\text{H}]^+$.

Cyclic Voltammograms of $\text{CpRe}(\text{P}(\text{Ar})_3)_2\text{H}_2$ Complexes. The initial scans in the cyclic voltammograms (CV) of complexes **1**, **3**, **4**, and **5** (as illustrated for **4** in Figure 1) from -0.5 to $+0.5$ V (vs. SCE) are all characterized by reversible one-electron processes in both dichloromethane and acetonitrile with the ratio of the anodic and cathodic currents (i_p^a/i_p^c) ranging between 1.0 and 1.2, provided the scan is reversed at $+0.5$ V (vs. SCE). The anodic and cathodic peak separations ($E_p^a - E_p^c$) are 60 mV in acetonitrile and approach 60 mV in dichloromethane with decreasing scan rate. A plot of i_a against the square root of the scan speed was linear for all complexes across a range of $20\text{--}500 \text{ mV s}^{-1}$ (correlation coefficient >0.99), as expected for a diffusion-controlled electrode process.¹¹ The data for peak potentials and current ratios are compiled in Table I. The ferrocene-ferrocenium couple was used as a known one-electron standard for these studies.¹²

The reversible waves observed in the cyclic voltammograms of the rhenium complexes correspond to the one-electron process in eq 4.



The magnitude of the reversible oxidation potentials E^0 listed in Table I is a function of the σ -donating or withdrawing abilities of the substituents¹³ in the triarylphosphine. A plot of E^0 in acetonitrile against σ_p as shown in Figure 2a is linear with a ρ value of 0.81 and a correlation coefficient of 0.993. This is consistent with E^0 becoming more positive as the donating ability of the phosphine decreases.

(11) Bard, A. J.; Faulkner, L. R. *Electrochemical Methods*; Wiley: New York, 1980.

(12) Collman, J. P.; Hegedus, L. S. *Principles and Applications of Organotransition Metal Chemistry*; University Science: Mill Valley, CA, 1980.

(13) Ritchie, C. D.; Sager, W. F. *Prog. Phys. Org. Chem.* **1964**, *2*, 323.

(14) Klingler, R. J.; Huffman, J. C.; Kochi, J. K. *J. Am. Chem. Soc.* **1980**, *102*, 208.

Table II. CV Parameters and Current Efficiencies (m/n) at More Anodic Potentials for $\text{CpRe}(\text{PAR}_3)_2\text{H}_2$ Complexes^a

entry	compd	solvent	$E_p^{\prime a}$, V ^b	$E_p^{\prime\prime a}$, V ^b	$(E_p^{\prime a} - E_p^{\prime\prime c})/2$, V ^b	m/n^c
1	1	CH ₃ CN	0.51	0.835	0.805	8
2	1	CH ₂ Cl ₂	0.62			12
3	3	CH ₃ CN	0.45	0.73	0.70	15
4	3	CH ₂ Cl ₂	0.54			20
5	4	CH ₃ CN	0.70	0.86	0.83	5
6	4	CH ₂ Cl ₂	0.97			16
7	5	CH ₃ CN	0.42	0.665	0.635	
8	5	CH ₂ Cl ₂	0.51			

^aSolutions were 5×10^{-4} M in the complex with 0.2 M TBAF as supporting electrolyte at a platinum disk electrode with a scan rate of 100 mV s⁻¹. ^bvs. SCE. ^cFrom controlled-potential electrolyses at $E_p^{\prime a}$.

Table III. Absorption Spectra for $\text{CpRe}(\text{PAR}_3)_2\text{H}_2$ Complexes and Their 17-Electron Radical Cations

compd	solvent	λ_{max} , nm (log ϵ)
1	CH ₃ CN	324 (3.81)
1	CH ₂ Cl ₂	326 (3.85)
1 ^{•+}	CH ₃ CN	395 (3.29)
1 ^{•+}	CH ₂ Cl ₂	405 (3.26)
3	CH ₂ Cl ₂	324 (3.78)
3 ^{•+}	CH ₂ Cl ₂	436 (3.33)
4	CH ₃ CN	313 (3.81)
4	CH ₂ Cl ₂	313 (3.83)
4 ^{•+}	CH ₃ CN	405 (3.29)
4 ^{•+}	CH ₂ Cl ₂	404 (3.08)

In CV scans allowed to go more positive than +0.5 V (vs. SCE), the first wave (potentials listed in Table I) becomes much less reversible ($i_p^a/i_p^c \gg 1$). Specifically, a second, irreversible oxidation of a much smaller anodic current than that observed in the first wave is observed at +0.5 to +1.0 V (vs. SCE) (Table II). However, entering the second oxidation results in a loss of reversibility of the first wave. The magnitude of $E_p^{\prime a}$ as shown in Figure 2b is again a function of the σ -donating or withdrawing ability of the substituents on the triarylphosphine ligands.

Continuing the CV scans in dichloromethane to more positive potentials beyond the second wave shows an irreversible oxidation of $E_p^{\prime a} > +1.4$ V (vs. SCE) for all four complexes, which is presumably multielectron from the magnitude of i_p^a . In acetonitrile, the anodic scans continued to more positive potentials beyond the second wave show a second reversible couple (Table II) with anodic and cathodic peak separations of 60 mV. The current passed in the second reversible couple is approximately half of the current passed in the first wave.

The magnitude of the reversible oxidation potentials E° listed in Table II is again a function of the σ -donating or withdrawing abilities of the substituents attached to the triarylphosphine in the complexes.¹³ A plot of E° against σ_p , as shown in Figure 2c for the second reversible wave in acetonitrile, is linear with a ρ value of 0.61 and a correlation coefficient of 0.999. The substituent effects are similar in the species responsible for both the first and second reversible waves, suggesting that both phosphine ligands are present in each.

Electrochemical Oxidations. Controlled-potential electrolyses of complex 1 in a standard divided cell at ambient temperature gave golden yellow solutions in both acetonitrile (λ_{max} 395 nm) and dichloromethane (λ_{max} 405 nm). Stirred-solution voltammograms of these solutions, after the passage of 0.95 faraday/mol, showed complete conversion of the oxidation wave that gives the radical cation of 1 to a reduction wave that regenerates 1 as determined by cyclic voltammetry (CV) and absorption spectroscopy. This is consistent with the formation of the radical cation by a one-electron oxidation as depicted in eq 4.

The species from the initial one-electron oxidations appear to be reasonably stable. The electrolyzed solutions of 1 could be left under an inert atmosphere in both acetonitrile and dichloromethane for 10 min without affecting the reversibility of the couple, suggesting that the 17-electron species is stable during the time frame of the experiment.

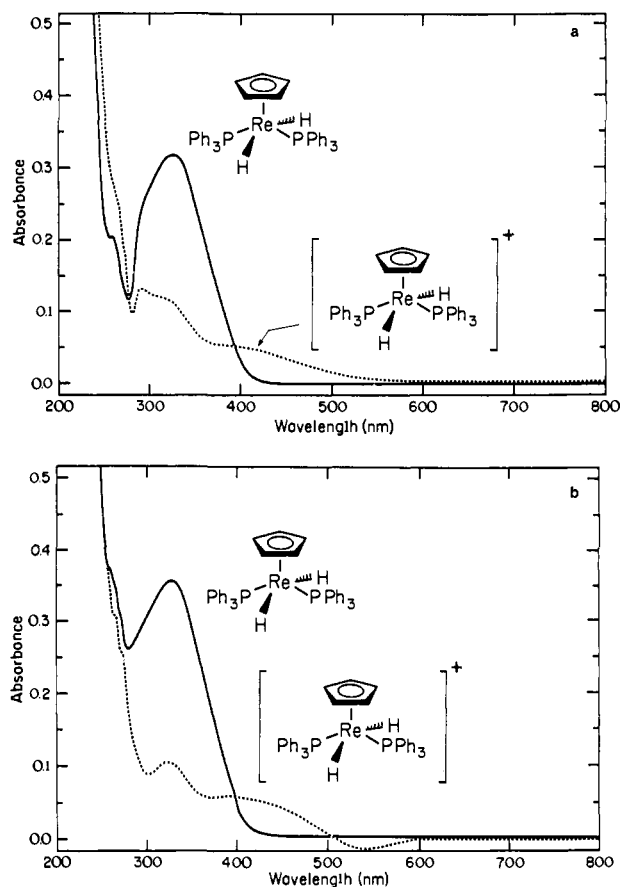


Figure 3. Absorption spectra of $\text{CpRe}(\text{PPh}_3)_2\text{H}_2$ (1) and $[\text{CpRe}(\text{PPh}_3)_2\text{H}_2]^{\bullet+}$ (1^{•+}) in (a) acetonitrile and (b) dichloromethane with 0.2 M tetrabutylammonium fluoroborate. The absorption spectra of 1^{•+} were obtained by oxidation of 1 at +0.5 V (vs. SCE) in an electrochemical thin-layer flow cell.

Using an electrochemical thin-layer flow cell, we obtained the absorption spectra of the oxidation products formed at +0.5 V (vs. SCE) at ambient temperature for complexes 1, 3, and 4. Appropriate spectral parameters are compiled in Table IV. Typical absorption spectra are shown for 1 in Figure 3.

To determine the reversibility of the system (oxidation to the radical cation and reduction back to the neutral starting complex), the thin-layer cell was used for the electrolyses and the results were analyzed by double-potential chronocoulometry. Complete oxidation of a dichloromethane solution of 1 at ambient temperature at +0.5 V (vs. SCE) required 0.91 faraday/mol, and the reduction of the oxidized starting material at 0.0 V (vs. SCE) resulted in the passage of 0.81 faraday/mol. Similarly, complete oxidation of an acetonitrile solution of 4 at +0.6 V (vs. SCE) required the passage of 0.99 faraday/mol while reduction of the oxidized starting material required 0.94 faraday/mol. These results indicate that, on the time scale of the experiment (1 mV s⁻¹ scan rate), the 17-electron radical cation intermediates are reasonably stable.

We next examined the observed loss of reversibility upon entering the second oxidation. From the current magnitude in the CV scans, it appeared that the species formed in the second wave was catalyzing the disappearance of the first wave. Controlled-potential electrolysis of an acetonitrile solution of 1 at +0.35 V (vs. SCE) reached a current plateau after the passage of 0.95 faraday/mol. A CV scan of the oxidized solution showed the reversible couple with E° at +0.25 V (vs. SCE) with the same current amplitude as the CV scan of the starting solution. The applied potential was increased to +0.6 V (vs. SCE). A second current plateau was reached in approximately 10 min after the passage of an additional 0.12 faraday/mol. CV scans of this oxidized solution showed no trace of either the initial one-electron couple with $E^\circ = 0.23$ V (vs. SCE) or the irreversible oxidation

Table IV. Summary of Crystallographic Data

crystal parameters	
formula	$\text{ReP}_2\text{NC}_{43}\text{H}_{40}$
fw	963.92
cryst system	monoclinic
space group	$P2_1/c$
Z	4
a, Å	9.908 (2)
b, Å	21.546 (9)
c, Å	18.967 (6)
β , deg	99.12 (2)
vol, Å ³	3997.7 (4.0)
d_{calcd} , g/cm ³	1.603
cryst dimens, nm	$0.21 \times 0.25 \times 0.30$
temp, °C	25
diffractometer	Enraf-Nonius CAD4, geometry
radiation (monochromator)	Mo, 0.71073 Å (graphite)
scan type	$2\theta/\omega$
scan rate, deg/min	2-16.5
total background time	scan time/2
takeoff angle, deg	2.6
scan range, deg	$0.6 + 0.35 \tan \theta$
2θ range, deg	4-42
data collected	$+h, +k, \pm l$
no. of data collected	4733
no. of unique data $> 3\sigma$	3066
no. of parameters varied	487
absorption coeff, cm ⁻¹	32.59
systematic absences	$0k0, k \text{ odd}; h0l, l \text{ odd}$
absorption correction	none
equivalent data	$0kl = 0k\bar{l}$
agreement between equiv data (F_{obsd})	0.030
R_1	0.0452
R_2	0.0538
goodness of fit	1.85

with $E_p^a = 0.51$ V (vs. SCE), but they showed only the second reversible wave with $E^\circ = 0.805$ V (vs. SCE). This result suggested that product formed in the second oxidation [$E_p^a = 0.51$ V (vs. SCE)] catalyzed the disappearance of **1** to give a new product [$E^\circ = 0.805$ V (vs. SCE)] with a current efficiency of at least 8 where the current efficiency (m/n) is defined as the number of moles of $\mathbf{1}^{*+}$ converted to the new product per faraday of electrons.

Similar results were obtained with use of the thin-layer flow cell illustrated in Figure 4. As the applied potential is reversed at more positive potentials, more $\mathbf{1}^{*+}$ has been lost than would be expected for the current under the curve for the continued positive scan (Figure 4, b compared to a). In Figure 4c, the total loss of the waves associated with **1** and of the bump for the second irreversible oxidation by the continued positive scan, as well as the appearance of a new, reversible couple, is apparent.

Complexes **3** and **4** gave similar results in controlled-potential electrolyses in both a standard cell and the thin-layer flow cell. Current efficiencies of between 5 and 20 were realized with the electrocatalysis of the disappearance of $\mathbf{3}^{*+}$ in dichloromethane being most efficient (Table II).

Chemical Oxidations. We sought to identify the products of oxidation of the rhenium complexes by product analysis of ferrocenium hexafluorophosphate (**6**)¹² oxidations of **1**. The one-electron couple of **6** in acetonitrile has $E^\circ = +0.355$ V (vs. SCE) making the oxidant compatible with E° values from Table I for the rhenium complexes. Furthermore, the reduction product of **6**, ferrocene, is very soluble in nonpolar solvents.

The addition of 1 equiv of **6** to an acetonitrile solution of **1** resulted in the complete disappearance of **1** from the reaction mixture, which gave three products that could be isolated as crystalline solids. One product which gave CV scans (Figure 5b) identical with the second reversible wave for **1** in acetonitrile [$E^\circ = 0.805$ V (vs. SCE) Figure 5a)] was isolated in 43% yield. The structure of this compound was identified as $[\text{CpRe}(\text{PPh}_3)_2(\text{NCCH}_3)\text{H}]^+[\text{PF}_6]^-$ (**7**) by elemental analysis, by ¹H NMR spectroscopy [acetone-*d*₆: δ 7.46 (m, 30 H), 4.68 (s, 5 H), -5.97 (t, 3 H, $J = 41.4$ Hz)], and unequivocally by single-crystal X-ray

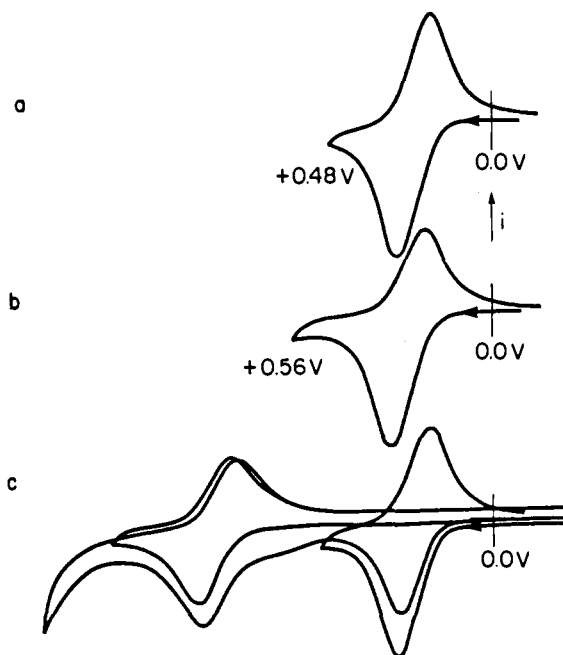


Figure 4. Thin-layer cyclic voltammogram of a 5.0×10^{-4} M solution of **1** in acetonitrile with 0.2 M tetrabutylammonium fluoroborate as supporting electrolyte between (a) 0.0 and 0.48 V, (b) 0.0 and 0.56 V, and (c) 0.0 and 1.3 V at 1 mV s^{-1} .

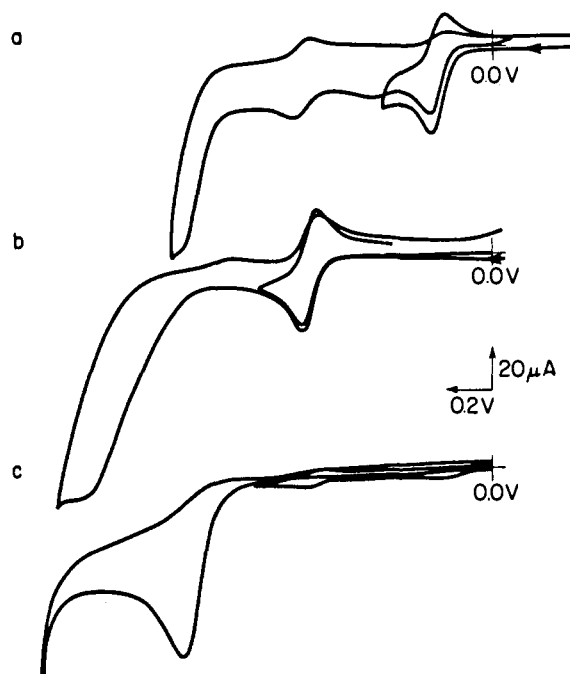


Figure 5. Cyclic voltammograms of 5×10^{-4} M solutions of (a) $\text{CpRe}(\text{PPh}_3)_2\text{H}_2$ (**1**), (b) $[\text{CpRe}(\text{PPh}_3)_2(\text{NCCH}_3)\text{H}]^+[\text{PF}_6]^-$ (**7**), and (c) $[\text{CpRe}(\text{PPh}_3)_2\text{H}_3]^+[\text{PF}_6]^-$ (**8**) in acetonitrile with 0.2 M tetrabutylammonium fluoroborate as supporting electrolyte at a platinum disk electrode and a scan rate of 0.1 V s^{-1} .

crystallographic analysis (vide infra). A second product was isolated in 45% yield and was identified as the known complex^{10a} $[\text{CpRe}(\text{PPh}_3)_2\text{H}_3]^+[\text{PF}_6]^-$ (**8**) by elemental analysis and ¹H NMR spectroscopy [CD_3CN : δ 7.5-7.3 (m, 30 H), 4.68 (s, 5 H), -5.97 (t, 3 H, $J = 30.1$ Hz)]. The CV scans of **8** (Figure 5c) were characterized by an irreversible 2-electron oxidation with $E_p^a = +1.38$ V (vs. SCE), which corresponds to an irreversible wave observed in the CV scans of **1** in acetonitrile (Figure 1). The third product was isolated in 6% yield as a bright red crystalline solid. This product was identified as $[\text{CpRe}(\text{NCCH}_3)_4]^{2+}2[\text{PF}_6]^-$ (**9**) by elemental analysis, ¹H NMR spectroscopy [CD_2Cl_2 : δ 5.58 (s, 5 H), 1.70 (s, 12 H)], and IR spectroscopy (KBr: 2302, 2283,

829 cm⁻¹). Compound **9** does not appear to be a primary product from the oxidation of **1** in acetonitrile (*vide infra*).

Compound **8** was prepared in an alternative manner by addition of aqueous HPF₆ to an ether slurry of **1**. The white powder was spectroscopically identical with **8** and analyzed correctly for the required molecular formula. The tetrafluoroborate salt of **8** was prepared as well and analyzed correctly by incorporating one water of crystallization into the molecular formula.

When the ferricinium oxidation of **1** was conducted in acetonitrile-*d*₃, the product mixture could be examined directly by ¹H NMR spectroscopy. Immediately following oxidation, the hydride region of the NMR spectrum displayed the 3:1 integral of the δ -5.97, to -9.13 triplets expected from a 1:1 mixture of **7** and **8**. A third product, present as ~6% of the product mixture, was tentatively identified as CpRe(PPh₃)(NCCD₃)H₂ (**10**) from signals at δ 4.93 (s, 5 H) and -9.43 (d, 2 H, *J* = 48.8 Hz). We were unsuccessful in our attempts to isolate **10**. None of the dication **9** was detected by ¹H NMR immediately after oxidation.

The product distribution in solution changed as a function of time. Although the relative amounts of **7** and **10** appeared to remain constant, the signals associated with **8** decreased with time, disappearing after 48 h. The signals associated with **7** and **10** decreased with time as well although at a slower rate. The cyclopentadienyl singlet for **9** increased with time, suggesting that **9** is indeed a secondary product produced after oxidation.

In view of the fact that the product mixture was not static in acetonitrile, the stability of the individual products **7** and **8** to the conditions of reaction was next investigated. Of particular concern was the possibility of the fortuitous formation of equal amounts of **7** and **8** by some secondary reaction. The ¹H NMR spectrum of an acetonitrile-*d*₃ solution of **7** was unchanged after 48 h at ambient temperature. However, trihydride **8** slowly reacted in acetonitrile solution to give initially **7** and **10** in a 3-to-2 ratio by ¹H NMR. At ambient temperature (22 °C), the half-life of **8** in acetonitrile was ~24 h; at 40 °C, the half-life was ~7 h. Attempts to monitor the kinetics of the disappearance of **8** showed that it was a non-first-order process with an increasing rate of disappearance with time, suggesting catalysis by some species formed during the reaction. Added **7** had no effect on the initial rate of disappearance of **8** at either 22 or 40 °C. Both **7** and **10** were also reactive in the reaction mixture containing **8**, presumably giving **9** and at least two other compounds (in approximately 10% yield) identified as triphenylphosphine and a new organometallic species with a broad hydride resonance at δ -0.35 and a cyclopentadienyl singlet at δ 5.99. The latter minor species was not characterized further.

In dichloromethane, oxidation of **1** with **6** gave only trihydride **8** which was isolated in 55% yield. When the oxidation was conducted in dichloromethane-*d*₂, the cyclopentadienyl and hydride protons of **8** integrated in a 5:3 ratio, suggesting that solvent was not the source of the third hydride ligand acquired in the oxidation of **1** to **8**.

The product studies were repeated with rhenium complex **4** in both acetonitrile and dichloromethane. In dichloromethane, ferricinium oxidation gave only one product, [CpRe(P(*p*-FC₆H₄)₃)₂H₃]⁺[PF₆]⁻ (**11**), produced in 46% yield and identified by its ¹H NMR spectrum [CD₃CN: δ 7.4 (m, 12 H), 7.23 (t, 12 H, *J* = 9 Hz), 4.99 (s, 5 H), -6.00 (t, 3 H, *J* = 31.5 Hz)]. In acetonitrile, ferricinium oxidation of **4** gave equal amounts of **11** and the acetonitrile substitution product, [CpRe(P(*p*-FC₆H₄)₃)₂(NCCCH₃)H]⁺[PF₆]⁻ (**12**). The product mixture from the oxidation of **4** was much less reactive toward further reaction with acetonitrile than the product mixture derived from the oxidation of **1**. The structure of complex **12** was assigned from its ¹H NMR spectrum (CD₃CN: δ 7.4 (m, 12 H), 7.15 (t, 12 H, *J* = 9 Hz), 4.70 (s, 5 H), -9.23 (t, 1 H, *J* = 42 Hz), the singlet from the coordinated NCCCH₃ was obscured).

The trihydride **11** was prepared by the addition of HPF₆ to an ether slurry of **4**. The ¹H NMR spectra of the white powder isolated in 82% yield from the reaction and **11** were identical.

X-ray Crystal Structure of 7. As mentioned above, identification of the species whose couple appeared at +0.805 V (vs. SCE) in

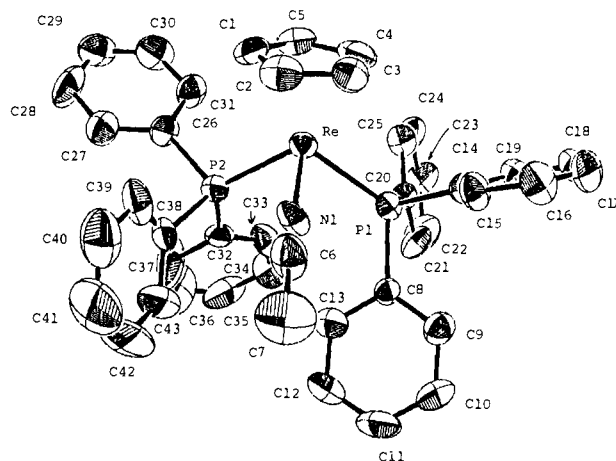


Figure 6. ORTEP drawing of [CpRe(PPh₃)₂(NCCH₃)H]⁺[PF₆]⁻ (**7**). Ellipsoids are shown at the 50% probability level.

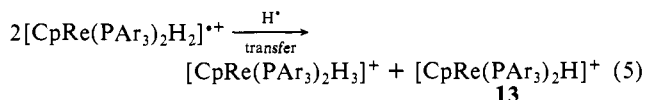
Table V. Selected Distances (Å) and Angles (deg) for [CpRe(PPh₃)₂(NCCH₃)H]⁺[PF₆]⁻ (**7**)

bond	distance	bond	angle
Re-P1	2.357 (2)	P1-Re-P2	108.68 (2)
Re-P2	2.369 (3)	P1-Re-cen ^a	125.7 (1)
Re-N1	2.074 (8)	P2-Re-cen ^a	123.1 (1)
N1-C6	1.101 (12)	N1-Re-cen ^a	114.0 (1)
C6-C7	1.54 (2)	P1-Re-N1	83.1 (2)
		P2-Re-N1	85.6 (2)

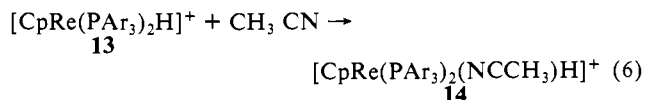
^acen is the C₅H₅ centroid.

acetonitrile was accomplished by crystallization of the material from acetonitrile upon oxidation of **1** with ferricinium. Standard data collection and reduction were carried out in accord with the parameters in Table IV. Patterson map solution of the structure showed the presence of a *trans*-CpRe(PPh₃)₂ moiety along with three small peaks (3-4 e⁻/Å³) arranged in a linear fashion away from the rhenium. These refined successfully as an acetonitrile ligand. The hydride ligand could not be located on the final difference Fourier map. Figure 6 shows an ORTEP plot of the molecule, Table V gives selected bonds and angles, and Table VI (available as supplementary material) lists fractional atomic coordinates.

Mechanistic Considerations in Acetonitrile. The CpRe-(PAR₃)₂H₂ complexes form stable 17-electron radical cations upon oxidation. The removal of a second electron from the radical cation generates a new product [CpRe(PAR₃)₂H₂]²⁺ that catalyzes the formation of two new species from the 17-electron radical cations. Ferricinium is a strong enough oxidant to remove the second electron. Formally, a hydrogen atom transfer from one radical cation to another as shown in eq 5 would generate the trihydride (i.e., **8** and **11**), a coordinatively saturated compound, and a monohydride species **13**, a coordinatively unsaturated intermediate.



The addition of a new ligand to **13** (eq 6) would then give the observed substitution product **14**.



The stability of the 17-electron species during the electrochemical oxidations suggests that hydrogen atom transfer is slow on this time scale. However, oxidation of the 17-electron Re(IV) compound gives a 16-electron Re(V) dication **15** which leads to a rapid disappearance of the 17-electron compound by ETC. Presumably, the formation of **15** facilitates either proton transfer

We cannot distinguish between hydrogen atom and proton transfer although both paths have precedent in the literature of the decomposition of organometallic radical cations.^{14,15} While these precedents do not involve ETC, they serve to illustrate the viability of both pathways in the disproportionation of the rhenium radical cations. Moreover, the chemistry of $(dmpe)_2(CO)_2TaH^+$ is strikingly similar to that of the $[CpRe(PAr_3)_2H_2]^{+}$ complexes in that while the radical cation is stable on the CV time scale, further oxidation to a dication generates an unstable species. The magnitude of E° for the reversible one-electron $Re(III)-Re(IV)$ couples depicted in eq 4 and 10 is similarly affected by substituents in the phosphine ligands. From strictly inductive arguments, the value of E° becomes more positive as the phosphine becomes less donating. Furthermore, the correlation is linear with respect to σ_p substituent constants (Figures 2 and 3).

The isolation of a 17-electron species from either the neutral or the acetonitrile-substituted rhenium complexes is currently being pursued. ESR and X-ray crystallographic characterization of such species would help in the understanding of these ETC reactions.

The substitution of acetonitrile for a hydride ligand in the $CpRe(PAr_3)_2H_2$ complexes complements the photochemical substitution reactions of these complexes^{9a} in which a phosphine ligand is lost. The behavior of these new complexes as catalysts for C-H bond activation is being investigated as are further substitution reactions of the radical cation species.

Experimental Section

Dichloromethane was dried over activity I alumina before use. Acetonitrile was distilled from P_2O_5 and stored over 3A molecular sieves. Tetrabutylammonium fluoroborate was obtained from Southwestern Analytical Chemicals, Inc., and was recrystallized from ethyl acetate-ether and dried at 80 °C under vacuum prior to use. UV-visible absorption spectra were obtained with a Hewlett-Packard 8450A spectrophotometer, scanning 200–800 nm with a 1-s acquisition time. ¹H NMR spectra were recorded on a General Electric QE-300 instrument. All manipulations of complexes during their syntheses and solvents were conducted by using standard glovebox and Schlenk techniques. Solvents were degassed under nitrogen and purified by distillation from standard drying agents.

The ligands $P(p-MeC_6H_4)_3$, $P(p-FC_6H_4)_3$, and $P(p-MeOC_6H_4)_3$ were purchased from Strem and were used as received.

Electrochemical Studies. A Princeton Applied Research Model 173 potentiostat/galvanostat, a Model 175 waveform generator, and a Model 179 current-voltage converter were used for the electrochemical experiments. The working electrode for cyclic voltammetry was a platinum disk (Princeton Applied Research). The porous electrode used for double-potential step chronocoulometry and for UV-visible spectrophotometry was similar to that reported by Miner and Kissinger¹⁷ except that a reticulated glassy carbon (RVC) tube was substituted for the carbon particles used by those authors. In a nonflow mode, the porous electrode exhibited thin-layer behavior with the cell volume being obtained by using tritolyamine as a known one-electron reversible oxidation. The RVC was obtained from Normar Industries and was of porosity 100, grade 4. A standard calomel reference electrode was used in all electrochemical measurements. To obtain the UV-visible spectra for the products of electrolysis, the exit of the electrochemical flow cell was connected to the quartz spectral flow cell with Omnifit 1/16 in. Teflon tubing and Tefzel connectors. All spectra were recorded while solutions were flowing through the electrolysis cell and the UV-visible cell.

X-ray Structural Determination of $[CpRe(PPH_3)_2(NCCH_3)H]^+[PF_6]^-$ (7). Well-formed crystals of the complex were grown by slow evaporation of a saturated acetonitrile solution of 7 in an inert N_2 atmosphere, washed with cold acetonitrile, and dried with circulating N_2 . Following mounting of the crystal with epoxy on a glass fiber, lattice constants were obtained from 25 centered reflections with values of X between 0° and 60°. Cell reduction with the program TRACER revealed the monoclinic crystal system. Data were collected on the crystal in accord with the parameters listed in Table V. The unique monoclinic space group $P2_1/c$ was assigned on the basis of systematic absences. Patterson map determination of the rhenium position allowed solution of the structure, and subsequent difference Fourier and full-matrix least-squares refinement converged to the final solution. Phenyl and cyclopentadienyl hydrogen atoms were placed in idealized positions with the program HYDRO and no attempt was made to place the three methyl hydrogens. A final

difference Fourier map and peak search failed to show any peaks near the metal in proper position to be the hydride ligand. Final anisotropic refinement of all non-hydrogen atoms was carried out with fixed positional and thermal ($\beta = 5.0$) parameters for the hydrogen atoms. The Molecular Structure Corporation SDP package was used for solution and refinement of the structure.¹⁸ Table V contains the relevant bond distances and angles, and Table VI includes the positional parameters.

Preparation of $O=ReCl_3[P(p-MeC_6H_4)_3]_2$. To 2.5 g (8.0 mmol) of an 85% solution of $HReO_4$ was added 3.5 mL of concentrated HCl. The resulting solution was added to 10 g (33 mmol) of $P(p-MeC_6H_4)_3$ in 100 mL of acetic acid. The resulting mixture was stirred for 1 h at ambient temperature. The product was collected by filtration, washed with acetic acid (50 mL) and ether (6 × 25 mL), and dried under vacuum to give 6.3 g (85%) of $O=ReCl_3[P(p-MeC_6H_4)_3]_2$ as a lime-green powder, mp 256–262 °C.

Anal. Calcd for $C_{42}H_{42}Cl_3OP_2Re$: C, 55.0; H, 4.6; P, 6.8. Found: C, 54.6; H, 4.6; P, 6.9.

Preparation of $O=ReCl_3[P(p-FC_6H_4)_3]_2$. To 2.5 g (8.0 mmol) of an 85% solution of $HReO_4$ was added 3.5 mL of concentrated HCl. The resulting solution was added to 10 g (32 mmol) of $P(p-FC_6H_4)_3$ in 100 mL of acetic acid. The resulting mixture was stirred for 1 h at ambient temperature. The product was collected by filtration, washed with acetic acid (50 mL) and ether (6 × 25 mL), and dried to give 5.55 g (73%) of $O=ReCl_3[P(p-FC_6H_4)_3]_2$ as a lime-green powder.

Anal. Calcd for $C_{36}H_{24}Cl_3F_6OP_2Re$: C, 45.9; H, 2.6; F, 12.1; P, 6.6. Found: C, 46.2; H, 2.9; F, 11.7; P, 6.6.

Preparation of $O=ReCl_3[P(p-MeOC_6H_4)_3]_2$. Tris(*p*-methoxyphenyl)phosphine (4.0 g, 11 mmol) was added to a slurry of $O=ReCl_3(PPh_3)_2$ in 100 mL of toluene. The resulting mixture was stirred at ambient temperature for 15 h. The product was collected by filtration, washed with ether (3 × 25 mL), and dried to give 1.85 g (67%) of $O=ReCl_3[P(p-MeOC_6H_4)_3]_2$ as a burnt-orange powder.

Anal. Calcd for $C_{42}H_{42}Cl_3O_7P_2Re$: C, 49.8; H, 4.2; P, 6.1. Found: C, 50.4; H, 4.3; P, 6.1.

General Procedure for the Preparation of $H_7Re(PAr_3)_2$ Complexes.

Preparation of $H_7Re[P(p-MeC_6H_4)_3]_2$. Lithium aluminum hydride (0.19 g, 5.0 mmol) was added in two portions to a slurry of $O=ReCl_3[P(p-MeC_6H_4)_3]_2$ in 25 mL of ether under a nitrogen atmosphere at ambient temperature. After being stirred for 1 h, the reaction mixture had changed color from lime-green to white. The reaction mixture was cooled to 0 °C under nitrogen and 0.25 mL of a 10% sodium hydroxide solution was carefully added, followed by 0.25 mL of water. The reaction mixture was filtered through a coarse glass frit. The filter cake was washed with 25 mL of ether. The combined filtrates were concentrated. The addition of 20 mL of ether to the residue and subsequent chilling precipitated the product. The product was collected by filtration, washed with ether (4 × 5 mL), and dried to give 0.59 g (49%) of $H_7Re[P(p-MeC_6H_4)_3]_2$.¹⁹

Anal. Calcd for $C_{42}H_{49}P_2Re$: C, 62.9; H, 6.2; P, 7.7. Found: C, 62.3; H, 6.0; P, 7.6.

For $H_7Re[P(p-FC_6H_4)_3]_2$:^{9c} 33%; ¹H NMR (C_6D_6) δ 7.53 (m, 12 H), 6.66 (t, 12 H, $J = 8.5$ Hz), -4.43 (t, 7 H, $J = 18.4$ Hz). Anal. Calcd for $C_{36}H_{31}F_6P_2Re$: C, 53.2; H, 3.8. Found: C, 52.6; H, 3.9.

For $H_7Re[P(p-MeOC_6H_4)_3]_2$: 67%. Anal. Calcd for $C_{42}H_{49}O_6P_2Re$: C, 56.2; H, 5.5; P, 6.9. Found: C, 56.4; H, 5.4; P, 7.0.

General Procedure for the Preparation of $CpRe(PAr_3)_2H_2$ Complexes.

Preparation of $CpRe[P(p-FC_6H_4)_3]_2$ (4). Tetrahydrofuran (5 mL) and freshly cracked cyclopentadiene (1 mL) were condensed into a tube containing $H_7Re[P(p-FC_6H_4)_3]_2$ (0.70 g, 0.84 mmol). The reaction mixture was sealed under vacuum and was placed in an 82 °C oil bath for 2 h. The tube was broken open, the reaction mixture was concentrated, and hexamethyldisiloxane (5 mL) was transferred to the residue. The resulting mixture was heated at 100 °C for 1 h and then was quickly filtered through a pad of Celite. The filter cake was washed with 2 mL of ether. The crystalline product was collected from the filtrate by filtration. The crystals were washed with 5 mL of cold hexane and dried to give 0.38 g (51%) of 4.^{10c} ¹H NMR (C_6D_6) δ 7.28 (d × d, 12 H, $J = 7.2$ Hz), 6.65 (t, 12 H, $J = 7.5$ Hz), 4.14 (s, 5 H), -10.30 (t, 2 H).

Anal. Calcd for $C_{41}H_{31}F_6P_2Re \cdot Et_2O$: C, 56.3; H, 4.3; P, 6.5. Found: C, 56.3; H, 4.3; P, 6.5.

For 3:^{9c} 22%; ¹H NMR (C_6D_6) δ 7.67 (d, 12 H, $J = 7.2$ Hz), 6.90 (d, 12 H, $J = 7.2$ Hz), 4.39 (s, 5 H), 2.04 (s, 18 H), -9.91 (t, 2 H), 22%. Anal. Calcd for $C_{47}H_{49}P_2Re$: C, 65.5; H, 5.7. Found: C, 65.4; H, 5.5.

(18) $R_1 = \{ \sum |F_o| - |F_c| \} / \{ \sum |F_o| \}$; $R_2 = \{ \sum w(|F_o| - |F_c|)^2 \}^{1/2} / \{ \sum w F_o^2 \}$; where $w = [\sigma^2(F_o) + [F_o^2]]^{-1/2}$ for the non-Poisson contribution weighting scheme. The quantity minimized was $\sum w(|F_o| - |F_c|)^2$. Source of scattering factors f_o, f', f'' : Cromer, D. T.; Waber, J. T. *International Tables for X-Ray Crystallography*; The Kynoch Press: Birmingham, England, 1974; Vol. IV, Tables 2.2B and 2.3.1.

(17) Miner, D. J.; Kissinger, P. T. *Biochem. Pharmacol.* **1979**, *28*, 3285.

(19) Fremi, M.; Giusto, D.; Romiti, P. *Gazz. Chim. Ital.* **1975**, *105*, 435.

For **5**: 44%; $^1\text{H NMR}$ (C_6D_6) δ 7.695 (d, 12 H, $J = 8.4$ Hz), 6.68 (d, 12 H, $J = 8.4$ Hz), 3.25 (s, 18 H), -9.89 (t, 2 H). Anal. Calcd for $\text{C}_{47}\text{H}_{49}\text{O}_6\text{P}_2\text{Re}$: C, 58.9; H, 5.2; P, 6.5. Found: C, 58.4; H, 4.9; P, 6.4.

For **1**: $^1\text{H NMR}$ (C_6D_6) δ 7.2 (m, 30 H), 4.27 (s, 5 H), -9.95 (t, 2 H).

Ferricinium Oxidation of $\text{CpRe}(\text{PPh}_3)_2\text{H}_2$ (1**).** **A. In Acetonitrile.** Compound **1** (0.428 g, 0.500 mmol) was dissolved in 20 mL of acetonitrile. Ferricinium hexafluorophosphate (0.166 g, 0.500 mmol) was added, giving an orange solution. The reaction mixture was chilled, precipitating a gold crystalline solid which was collected by filtration. The mother liquors were concentrated to half-volume which precipitated a second crop of the gold crystals. Combined yield was 0.198 g (43%) of $[\text{CpRe}(\text{PPh}_3)_2(\text{NCCH}_3)\text{H}]^+[\text{PF}_6]^-$ (**7**).

Anal. Calcd for $\text{C}_{43}\text{H}_{39}\text{N}_2\text{P}_2\text{Re}\cdot\text{PF}_6$: C, 53.6; H, 4.1; N, 1.5; P, 9.7. Found: C, 53.5; H, 4.1; N, 1.0; P, 9.2.

The mother liquors were diluted with 15 mL of ether. The resulting solution was chilled, precipitating a white crystalline solid. The solid was collected by filtration and dried to give 0.202 g (45%) of $[\text{CpRe}(\text{PPh}_3)_2\text{H}_3]^+[\text{PF}_6]^-$ (**8**).

Anal. Calcd for $\text{C}_{41}\text{H}_{38}\text{P}_2\text{Re}\cdot\text{PF}_6$: C, 53.3; H, 4.1; P, 10.1. Found: C, 53.0; H, 4.4; P, 10.0.

The mother liquors were allowed to stand 24 h, precipitating dark red crystals which were collected by filtration to give 0.022 g (6%) of $[\text{CpRe}(\text{NCCH}_3)_4]^{2+}2[\text{PF}_6]^-$ (**8**).

Anal. Calcd for $\text{C}_{13}\text{H}_{17}\text{N}_4\text{Re}\cdot 2\text{PF}_6$: C, 22.1; H, 2.4; N, 7.9. Found: C, 22.5; H, 2.8; N, 7.9.

B. In Acetonitrile- d_3 . Complex **1** (0.086 g, 0.10 mmol) was dissolved in 5 mL of acetonitrile- d_3 . The ferricinium hexafluorophosphate (0.033 g, 0.10 mmol) was added and the resulting mixture stirred at ambient

temperature for 3 min. Aliquots were then examined by $^1\text{H NMR}$.

C. In Dichloromethane. Complex **1** (0.214 g, 0.250 mmol) was dissolved in 10 mL of dichloromethane. Ferricinium hexafluorophosphate (0.083 g, 0.25 mmol) was added and the resulting solution stirred for 5 min at ambient temperature. The reaction mixture was concentrated to 5 mL and 15 mL of ether was added. The resulting solution was chilled, precipitating a white solid. The solid was collected by filtration to give 0.127 g (55%) of **8**.

Preparation of **8 from **1**.** To a slurry of **1** (0.17 g, 0.20 mmol) in 15 mL of ether was added a drop of 60% aqueous HPF_6 . A white solid precipitated immediately which was collected by filtration and washed with ether (6×10 mL). The $^1\text{H NMR}$ spectrum of the product was identical with that of **8**: (CD_3CN) δ 7.5-7.3 (m, 30 H), 4.68 (s, 5 H), -5.97 (t, 3 H, $J = 30.1$ Hz).

The tetrafluoroborate salt was prepared similarly with 50% aqueous HBF_4 . Anal. Calcd for $\text{C}_{41}\text{H}_{38}\text{P}_2\text{Re}\cdot\text{BF}_4\cdot\text{H}_2\text{O}$: C, 55.7; H, 4.6; P, 7.0. Found: C, 56.0; H, 4.7; P, 6.7.

Ferricinium Oxidation of $\text{CpRe}[\text{P}(p\text{-FC}_6\text{H}_4)_3]_2\text{H}_2$ (4**) in Acetonitrile- d_3 .** Complex **4** (0.090 g, 0.10 mmol) was dissolved in 2 mL of acetonitrile- d_3 . Ferricinium hexafluorophosphate (0.033 g, 0.10 mmol) was added and the reaction mixture examined by $^1\text{H NMR}$.

Acknowledgment. The authors thank Catherine Franke for her expertise in conducting the flow cell experiments and Alex Wernberg for helpful and stimulating discussions.

Supplementary Material Available: Table of fractional atomic coordinates (3 pages). Ordering information is available on any current masthead page.

Equilibria Studies Involving Ligand Coordination to "Open Titanocenes": Phosphine and Pentadienyl Cone Angle Influences and the Existence of These Electron-Deficient Molecules

Lothar Stahl and Richard D. Ernst*

Contribution from the Department of Chemistry, University of Utah, Salt Lake City, Utah 84112. Received November 25, 1986

Abstract: A series of phosphine adducts of bis(2,4-dimethylpentadienyl)titanium has been prepared, having the formulas $\text{Ti}(\text{2,4-C}_7\text{H}_{11})_2\text{L}$, for which $\text{L} = \text{P}(\text{C}_2\text{H}_5)_3$, $\text{P}(\text{OC}_2\text{H}_5)_3$, $\text{P}(\text{OCH}_3)_3$, $\text{P}(\text{CH}_3)_2(\text{C}_6\text{H}_5)$, and $\text{P}(\text{CH}_3)_3$. In solution these 16-electron adducts reversibly dissociate the phosphine or phosphite ligands, with respective ΔH values being 10.0, 10.6, 11.4, 12.9, and 14.5 kcal/mol, with the ΔS values falling in the range of 27.4-34.1 eu. Except for the seemingly weak binding by phosphites, these data can be rationalized in terms of reported ligand cone angles, and it is suggested that the cone angles for $\text{P}(\text{OMe})_3$ and a few related ligands should be revised, in some cases quite significantly. In addition, the $\text{P}(\text{C}_2\text{H}_5)_3$ adducts of $\text{Ti}(\text{3-C}_6\text{H}_9)_2$ and $\text{Ti}(\text{C}_5\text{H}_7)_2$ have been prepared ($\text{C}_6\text{H}_9 =$ methylpentadienyl; $\text{C}_5\text{H}_7 =$ pentadienyl). Similar studies indicate significantly enhanced phosphine binding, with ΔH and ΔS values being 14.6 kcal/mol and 34.8 eu for the former compound. For the latter complex, no detectable dissociation could be observed up to 60 °C, at which point decomposition took place. This information suggests that nonbonded repulsions between eclipsing pentadienyl methyl groups disfavor the formation of the ligand adducts, and hence they are to a large extent responsible for the isolability of the 14-electron "open titanocene", $\text{Ti}(\text{2,4-C}_7\text{H}_{11})_2$.

Of all the metallocenes, titanocene has exhibited perhaps the most intriguing chemistry, which includes applications in catalysis and organic synthesis.¹ Unlike the other $\text{M}(\text{C}_5\text{H}_5)_2$ complexes

from vanadium to nickel, $\text{Ti}(\text{C}_5\text{H}_5)_2$ is known to be extremely unstable, and all attempts to isolate this material have failed. In fact, a myriad of other materials have been isolated, including nitrogen adducts like $[\text{Ti}(\text{C}_5\text{Me}_5)_2]_2\text{N}_2$, and a variety of complexes containing ligands such as hydride, fulvalene, etc. Even $\text{Ti}(\text{C}_5\text{-}(\text{CH}_3)_2)_2$ is unstable, existing in equilibrium with a Ti(IV) complex which decomposes at room temperature.^{1d} Recently we reported the synthesis and characterization of an "open titanocene", bis-(2,4-dimethylpentadienyl)titanium, which contrasts markedly with "titanocenes" in being quite stable thermally despite its 14-electron configuration.^{2,3} Furthermore, this green compound does not form

(1) (a) Pez, G. P.; Armor, J. N. In *Advances in Organometallic Chemistry*; West, R., Stone, F. G. A., Eds.; Academic: New York, 1981; Vol. 19, p 1. (b) Bottrill, M.; Gavens, P. D.; McMeeking, J. In *Comprehensive Organometallic Chemistry*; Wilkinson, G., Stone, F. G. A., Abel, E. W., Eds.; Pergamon: Oxford, 1982; Vol. 3, pp 281-329. (c) Bottrill, M.; Gavens, P. D.; Kelland, J. W.; McMeeking, J. In *Comprehensive Organometallic Chemistry*; Wilkinson, G., Stone, F. G. A., Abel, E. W., Eds.; Pergamon, 1982; Vol. 3, pp 331-474. (d) Bercaw, J. E. *J. Am. Chem. Soc.* 1974, 96, 5087. (e) Tebbe, F. N.; Parshall, G. W.; Reddy, G. S. *Ibid.* 1978, 100, 3611. (f) Stille, J. R.; Grubbs, R. H. *Ibid.* 1983, 105, 1664. (g) Brown-Wensley, K. A.; Buchwald, S. L.; Cannizzo, L.; Clawson, L.; Ho, S.; Meinhardt, D.; Stille, J. R.; Straus, D.; Grubbs, R. H. *Pure Appl. Chem.* 1983, 55, 1733.

(2) (a) Liu, J.-Z.; Ernst, R. D. *J. Am. Chem. Soc.* 1982, 104, 3737. (b) Ernst, R. D.; Liu, J.-Z.; Wilson, D. R. *J. Organomet. Chem.* 1983, 250, 257.